Hexagonal diamond from single-walled carbon nanotubes

S. Reich*, P. Ordejón*, R. Wirth†, J. Maultzsch**, B. Wunder†, H.-J. Müller†, C. Lathe†, F. Schilling†, U. Dettlaff-Weglikowska‡, S. Roth‡ and C. Thomsen**

*Institut de Ciència de Materials de Barcelona (CSIC), Campus de la U.A.B., 08913 Bellaterra, Barcelona, Spain
†Geoforschungszentrum Potsdam, Div. 4, Telegrafenberg, 14473 Potsdam, Germany
**Institut für Festkörperphysik, Technische Universität Berlin, Hardenbergstr. 36, 10623 Berlin, Germany
‡Max-Planck-Institut für Festkörperforschung, Heisenbergstr. 1, 70569 Stuttgart, Germany

Abstract. We studied the transformation of single-walled carbon nanotubes into diamond by *ab-initio* calculations and high-pressure and temperature experiments. From the calculations we predict the formation of hexagonal diamond as a high-pressure nanotube phase. High-resolution TEM pictures of single-walled carbon nanotubes subjected to 9 GPa and 700°C clearly indicate the formation of hexagonal diamond grains.

The high-pressure phase diagram of carbon is dominated by diamond, which is energetically the most stable structure at pressures above ≈ 2 GPa. At ambient pressure graphite is the phase with the lowest total energy; however, the difference in total energy between the pure sp^2 and sp^3 phases is only some tens meV per carbon atom.[1] In contrast to the small difference in total energy, the energy barriers between graphite and diamond are well above 300 meV per carbon atom at ambient pressure.[1] They thus prevent a transformation of diamond into graphite even at very long time scales. To overcome these barriers high pressures and high temperature conditions have to be applied. It was shown that graphite and C_{60} transform into diamond at pressures $\approx$15 GPa and temperatures above 1000 K.[2, 3]

In this paper we report on the transformation of single walled carbon nanotubes into diamond. From *ab-initio* calculations we find that single-walled carbon nanotubes form a polymerized high pressure phase above ≈ 7 GPa. This phase transforms into hexagonal diamond by a succesive interlinking of the flattened nanotubes walls. We present high-resolution TEM pictures of single-walled carbon nanotubes which we subjected to high-pressures and temperatures. The interlayer distance of ≈ 4.1 Å observed after the high-pressure treatment clearly indicates the transition into the hexagonal diamond phase.

The basic building blocks of diamond are buckled hexagonal carbon planes. These planes can be arranged in an ABC stacking yielding cubic diamond, which is the phase normally simply called diamond [see Fig. 1(a)]. Similar to the wurzite structure in polar semiconductors, the buckled carbon planes can also be arranged in an ABAB stacking. This phase is called hexagonal diamond; it is shown in Fig. 1b). Hexagonal diamond was

CP685, *Molecular Nanostructures: XVII Int'l. Winterschool/Euroconference on Electronic Properties of Novel Materials,* edited by H. Kuzmany, J. Fink, M. Mehring, and S. Roth

discovered in graphite samples after shock-wave and high-pressure experiments.[4, 5, 6] High-pressure and temperature experiments on graphite sometimes yield cubic, sometimes hexagonal, or a mixture of the two diamond phases. The end product depended on the starting material and the high-pressures equipment in a not-fully understood way.[7, 8, 9, 10] Likewise, twinned cubic-hexagonal crystals were found in *ab-initio* molecular-dynamics calculations of the graphite to diamond transition.[11] It was suggested by Tateyama *et al.*[1] that the graphite to cubic diamond transitions requires a sliding of the graphene planes. In contrast hexagonal diamond results if a sliding of the layers is forbidden.

Single-walled carbon nanotubes are another potential source of artificial diamond. To study the high-pressure phases of single-walled carbon nanotubes and a possible transformation into diamond we performed *ab-initio* total energy calculations of (6,6) nanotube crystals. We used the SIESTA[12, 13] *ab-initio* package within the local density approximation[14] to relax the atomic coordinates of (6,6) nanotube crystals under applied hydrostatic pressure. The relaxations were done for pressures between 0 and 60 GPa by a conjugate gradient minimization under the constrained of an hydrostatic stress tensor. The minimization was considered converged if the forces on the atoms were below 0.04 eV/Å and every component of the stress tensor within $5-10$ % of the desired value. For the *ab-initio* calculation we replaced the core electrons by non-local norm-conserving pseudopotentials;[15] the valence electrons were described by a double-ζ polarized basis set.[13] The basis set cutoffs were 5.12 a.u. for the *s* orbital and 6.25 a.u. for the *p* and the polarizing *d* orbitals. In real space we used a grid energy cutoff of 250 Ry; in reciprocal space we included 64 *k* points.

At low pressures ($0-6$ GPa) the response of the nanotube crystal to an externally applied pressure is mainly governed by the weak van-der-Waals interaction between the tubes. We found a bulk modulus of 37 GPa in excellent agreement with high-pressure x-ray experiments on single-walled carbon nanotubes.[16] At a pressure of 7 GPa the circular tubes collapsed into a phase with an elliptical cross section. Although this phase requires a large strain energy in parts of the nanotube walls, it is favourable at high pressure, because the empty volume inside the tubes is reduced by 5 % compared to the circular phase at the same pressure. For larger diameter tubes the relative strain energy is much smaller. Thus this transition is expected to occur at lower pressures as suggested by piston-cylinder experiments.[17] At the point of strongest curvature of the nanotube

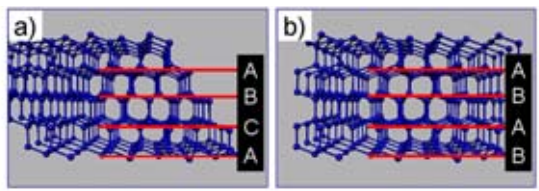

FIGURE 1. a) Cubic diamond with an ABC stacking of the carbon planes. This stacking is obtained by a translation within the carbon planes. b) Hexagonal diamond with an ABAB stacking. This stacking results from a rotation of every second plane by 180° around the axis perpendicular to the planes.

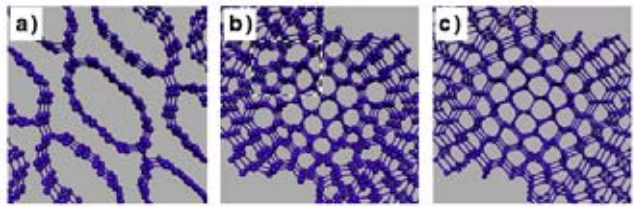

FIGURE 2. a) (6,6) nanotube crystal at 7.5 GPa pressure. The tubes have an elliptical cross section; diamond-like carbon-carbon bonds connect the tubes. b) (6,6) crystal at 40 GPa. At this pressure the tubes are transformed into a pure sp^3 phase. The dashed rectangular highlights the pentagon-heptagon defects. c) Hexagonal diamond structure obtained from b) by the rotation of one carbon bond per nanotube unit cell. Compare the picture to the ideal hexagonal diamond show in Fig. 1b).

wall the carbon-carbon bonds are of strongly mixed sp^2 and sp^3 character. The structure with an elliptical cross section was unstable when we further increased the pressure. Figure 2a) shows the relaxed structure at a pressure of 7.5 GPa. The flattened nanotubes are connected by carbon-carbon bonds which are almost purely of sp^3 character. In our calculation, the interlinked structure was stable when we released the pressure; evidence for the formation of this phase under pressure was also found in high-pressure and temperature experiments.[18]

Under a pressure of 40 GPa the flattened nanotube walls buckle and subsequently carbon-carbon bonds are formed between the nanotube walls. Finally, the tubes are transformed into the sp^3 structure shown in Fig. 2b). The difference between the high-pressure nanotube phase and the hexagonal diamond structure is the presence of pentagon-heptagon defects which are indicated by the dashed rectangular in Fig. 2b). If we rotate one carbon bond per nanotube unit cell we finally obtain a defect-free hexagonal-diamond crystal presented in Fig. 2c). We calculated the total energy at various pressures for the ambient pressure nanotubes, the pentagon-heptagon defect hexagonal diamond, and the defect-free diamond phase. At ambient pressure the hexagonal diamond with a 5-7 defect is by 80 meV per carbon atom lower in total energy than the crystal of circular nanotubes. The total energy is further reduced by 200 meV in the defect-free hexagonal-diamond phase. Once these phases are formed under high pressure, they are therefore stable under the release of pressure. We also estimated the transition barrier between the interlinked nanotube phase and hexagonal diamond by following the transition path obtained at 40 GPa at various lower pressure. This approach gives an upper bound for the energy barrier, since the saddle point at low pressure might be at a different point in the multi-dimensional phase space. At ambient pressure we found an energy barrier below 150 meV, which is by more than a factor of two lower than for the graphite to diamond transition (350 meV for graphite to cubic diamond and 415 meV for graphite to hexagonal diamond)[1]. The much lower transition barrier suggests that comparatively low pressures are required for transforming nanotubes into diamond at high temperatures. To test this prediction we performed high-pressure and temperature experiments on single-walled carbon nanotubes.

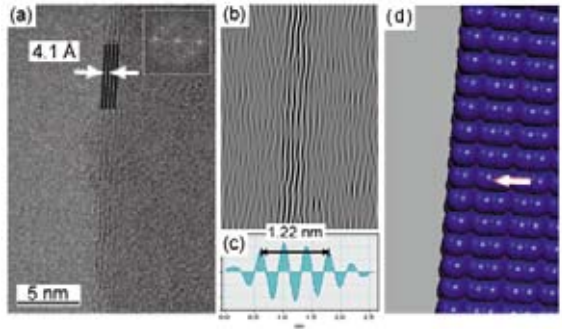

FIGURE 3. a) High-resolution TEM picture of the nanotube sample after high-pressure and high-temperature experiments. The lattice plains running from the top to the bottom of the picture indicate the presence of an hexagonal diamond grain (lattice spacing 4.1 Å). b) Inverse FFT of the lattice fringes in figure a); c) height profile of b). d) Schematic picture of an hexagonal diamond grain. The *c* axis with a lattice constant of 4.12 Å is indicated by the arrow.

The purified nanotubes were prepared by the laser-ablation method using Ni/Co catalysts. We subjected the tubes to a pressure of 9.0 GPa and 700°C in a MAX80 multi-anvil cell. First, the pressure was increased at room temperature up to 9.0 GPa followed by a heating of the sample to 700°C. Afterwards the sample was rapidly quenched to room temperature and, finally, the pressure was released. We characterized the samples before and after the high-pressure treatment with x-ray and Raman scattering, electron-energy loss spectroscopy and high-resolution transmission electron microscopy. A detailed account of the experiments will be published elsewhere; here we concentrate on the results of the TEM measurements, which indicate the formation of small grains of hexagonal diamond. The high-resolution energy filtered (zero loss) TEM images were obtained with a PHILLIPS CM200 transmission electron microscope equipped with a Lab6 electron source.

After the high-pressure run the samples mostly consisted of carbon nanotubes and some graphitic carbon with a lattice spacing of 3.4 Å. However, we found small grains of an sp^3 carbon phase, which were absent in the starting material or in samples subjected to lower pressures (up to 5 GPa). In Figure 3a) we show a TEM picture of such a spot. The lattice planes running from the top to the bottom in the picture (highlighted by the black lines) have an interlayer spacing of 4.1 Å. The planes are better visible in Fig. 3b) which shows an inverse Fourier transform of the FFT lattice fringes; part c) of the figure shows the height profile of the inverse FFT. Hexagonal diamond is the only carbon phase with sp^3 bonding and a lattice constant of 4.17 Å (along the *c* axis). Electron-energy loss spectra taken on the grains showed two separate peaks at 292 and 298 eV typical for the $p\sigma^*$ transitions in sp^3 bonded carbon.

The hexagonal-diamond grains we observed in the high-pressure sample typically consisted of only a few carbon layers along the *c* axis, but were several nm long (> 20 nm). Figure 3d) shows schematically shows an hexagonal-diamond crystal with

the same orientation as the grain in Fig. 3a). The large ratio between the length and the width of the grain suggests that after the transformation of the nanotubes the *c* axis of the hexagonal-diamond crystal is perpendicular to the *z* axis of the original nanotubes. Precisely this is the transformation path that we predicted from the *ab-initio* calculations.

In summary, form both our calculations and experimentally we found that single-walled carbon nanotubes transform into hexagonal as opposed to cubic diamond. Hexagonal diamond is favoured when using carbon nanotubes as the starting material, because of the polymerized nanotube phase, which forms at intermediate pressure. The carbon-carbon bonds between the tubes prevent a sliding of the flattended nanotubes walls. Further high-pressure experiments aiming at larger, more macroscopic diamond crystals are under way.

We were supported by the Ministerio de Ciéncia y Technología (Spain) and the DAAD (Germany) within the Acciones Intergradas Hispano-Alemanas. St.R. acknowledges a fellowship by the Akademie der Wissenschaften Berlin-Brandenburg. P.O. acknowledges the Fundación Ramon Areces, EU Project SATURN, and a Spain-DGI Project. J.M. was supported by the Deutsche Forschungsgemeinschaft (DFG). High-pressure experiments were performed at the HASYLAB Hamburg. Parts of the calculations were carried out at the CESCA and CEPBA supercomputing facilities.

REFERENCES

1. Tateyama, Y., Ogitsu, T., Kusakabe, K., and Tsuneyuki, S., *Phys. Rev. B*, **54**, 14994–15001 (1996).
2. Clarke, R., and Uher, C., *Adv. Phys.*, **33**, 469–566 (1984).
3. Blank, V. D., Buga, S. G., Dubitsky, G. A., Serebryanaya, N. R., Popov, M. Y., and Sundqvist, S., *Carbon*, **36**, 319–343 (1998).
4. Hannemann, R. E., Strong, H. M., and Bundy, F. P., *Science*, **155**, 995–997 (1967).
5. Bundy, F. P., and Kasper, J. S., *J. Chem. Phys.*, **46**, 3437–3446 (1967).
6. DeCarli, P. S., and Jamieson, J. C., *Science*, **133**, 1961 (1821-1822).
7. Endo, S., Idani, N., Oshima, R., Takano, K. J., and Wakatsuki, M., *Phys. Rev. B*, **49**, 22 (1994).
8. Zhao, Y. X., and Spain, I. L., *Phys. Rev. B*, **40**, 993 (1989).
9. Aust, and Drickames, *Science*, **140**, 3568 (1963).
10. Yagi, T., Utsumi, W., Yamakata, M.-A., Kikegawa, T., and Shimomura, O., *Phys. Rev. B*, **46**, 6031–6039 (1992).
11. Scandolo, S., Bernasconi, M., Chiarotti, G. L., Focher, P., and Tosatti, E., *Phys. Rev. Lett.*, **74**, 4015–4018 (1995).
12. Soler, J. M., et al., *J. Phys.: Condens. Matter*, **14**, 2745–2779 (2002).
13. Artacho, E., Sánchez-Portal, D., Ordejón, P., García, A., and Soler, J., *phys. stat. sol. (b)*, **215**, 809 (1999).
14. Perdew, J. P., and Zunger, A., *Phys. Rev. B*, **23**, 5048 (1981).
15. Troullier, N., and Martins, J. L., *Phys. Rev. B*, **43**, 1993 (1991).
16. Reich, S., Thomsen, C., and Ordejón, P., *Phys. Rev. B*, **65**, 153407 (2002).
17. Chesnokov, S. A., Nalimova, V. A., Rinzler, A. G., Smalley, R. E., and Fischer, J. E., *Phys. Rev. Lett.*, **82**, 343–346 (1999).
18. Khabashesku, V. N., et al., *J. Phys. Chem. B*, **106**, 11155–11162 (2002).